Design and Analysis of Truss Aerial Transportation System (TATS): The Lightweight Bar Spherical Joint Mechanism

Xiaozhen Zhang[1], Qingkai Yang[1], Rui Yu[1], Delong Wu[1], Shaozhun Wei[1], Jinqiang Cui[2], and Hao Fang[1]

***Abstract*— In aerial cooperative transportation missions, it has been recognized that for small-sized but heavy payloads, the cable-suspended framework is a preferred manner. However, to maintain proper safe flight distances, cables always stay inclined, which implies that horizontal force components have to be generated by UAVs, and only partial thrust forces are used for gravity compensation. To overcome this drawback, in this paper, a new cooperative transportation system named Truss Aerial Transportation System (TATS) is proposed, where those horizontal forces can be internally compensated by the bar spherical joint structure. In the TATS, rigid bars can powerfully sustain the desired distances among UAVs for safe flight, resulting in a more compact and effective transportation system. Thanks to the structural advantage of the truss, the rigid bars can be made lightweight so as to minimize their induced gravity burden. The construction method of the proposed TATS is presented. The improvement in energy efficiency is analyzed and compared with the cable-suspended framework. Furthermore, the robustness property of a TATS configuration is evaluated by computing the margin capacity. Finally, a load test experiment is conducted on our made prototype, the results of which show the effectiveness and feasibility of the proposed TATS.**

I. INTRODUCTION

A. Motivation

In recent years, Unmanned Aerial Vehicles (UAVs) have shown their potential in transportation tasks [1]-[2]. Multi-UAVs can carry heavier payloads than a single one, but in turn, the system structure and control become more complex. It can be divided into two categories according to the structure of the transportation system: cable-suspended framework and rigid framework.

The cable-suspended framework means the connections between the payload and UAVs are tethered cables, which is commonly adopted as the preferred solution for small-sized but heavy payloads. However, due to the inclined tensed cables, horizontal force components always exist for maintaining proper flight distances between UAVs. Only partial thrust generated by UAVs is used to compensate for the gravity effect of the payload, which leads to low energy efficiency.

The rigid framework means the connections between the payload and UAVs are rigid or by spherical and universal joints. It can avoid energy loss caused by horizontal force components in the cable-suspended framework, but the rigid framework requires the size of the payload should be large enough to place UAVs. For a small-sized but heavy payload, the rigid framework may not be applicable anymore.

Hence, the motivation of this paper is to develop a more efficient aerial transportation system for small-sized but heavy payloads. Inspired by the truss structure, the Truss Aerial Transportation System (TATS) is designed, which can overcome the profile limitation of the payload in rigid frameworks and energy loss from horizontal distance maintenance between UAVs in the cable-suspended frameworks. Furthermore, benefited from the inner-connected rigid bars, the integrated TATS can be compact in size.

B. Related work

Many research works about cable-suspended framework have been carried out including the inverse kinematics [3], payload tracking control [4], obstacle avoidance [5]-[6], formation-based transportation [7], and communication problem [8]. Apart from these, the energy consumption problem is studied in [9] using optimization technique. However, none of the above-mentioned works considers the energy efficiency from the perspective of mechanical structure improvement. The essential horizontal force components always exist along with inclined cables.

Another commonly used one is the rigid framework, where no inclined cables or horizontal force components exist, and UAVs can be directly attached to the payload [10] in a rigid manner. This integrated system constitutes a new aerial vehicle with the payload as the frame and UAVs as actuators. On the other hand, spherical [11] or universal [12] joints are used to connect the payload and UAVs. With these connecting mechanisms, the degrees of freedom is increased. The directions of thrusts related to the payload can also be changed so that the payload will be better operated. However, it is worth noting that regardless of the connection method between UAVs and the payload, the payload is always required to be large enough and high stiffness, so as to place UAVs and avoid destruction of the payload under the traction from UAVs. Therefore, the existing rigid framework is not applicable for small-sized but heavy payloads.

Trusses play a crucial role in modern engineering fields [13]. A truss structure consists of bar elements connected by pin joints to grow a rigid graph [14]. In a truss frame, no shearing force exists and all stresses are along the axial direction of bar elements, which allows the trusses to be manufactured with lightweight and strong mechanical structures using little material [15]. In addition, external forces on a truss joint can be distributed into the tensile network so

[1]Xiaozhen Zhang, Qingkai Yang, Rui Yu, Delong Wu, Shaozhun Wei, and Hao Fang are with the State Key Laboratory of Intelligent Control and Decision of Complex System, School of Automation, Beijing Institute of Technology, Beijing 100081, China. qingkai.yang@bit.edu.cn

[2]Jinqiang Cui is with the Department of Mathematics and Theories, Peng Cheng Laboratory, Shenzhen 518055, China.

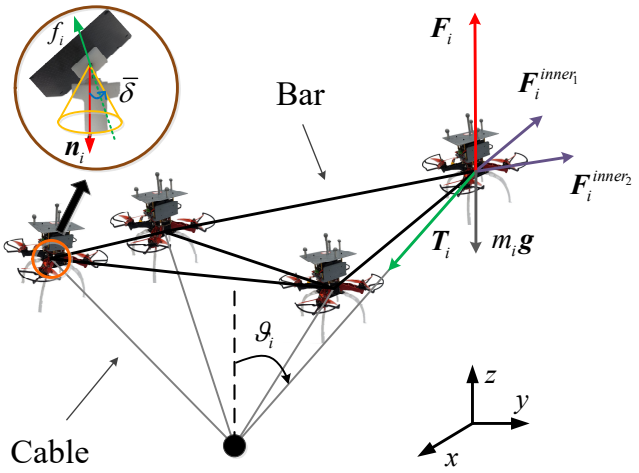

Fig. 1. Overview of the Truss Aerial Transportation System (TATS).

that the mechanical strength of a single bar element can be reduced [16]. Because of those structural advantages, truss structure has been applied in robotics, such as tensegrity robot [17], joint design [18], and protective structure design [19]. According to the best of our knowledge, no research has been reported yet on the application of trusses to aerial cooperative transportation.

C. Contribution

In this paper, a new aerial cooperative transportation system TATS is proposed, which enjoys the superior properties of the truss structure resulting in a compact and effective transportation system, especially targeting small-sized but heavy payloads. The high energy efficiency is verified in comparison with the cable-suspended framework when carrying a heavy payload. In addition, the robustness of the TATS configuration is analyzed in terms of capacity margin. All the theoretical results are further tested on the prototype system.

The remainder of this paper is organized as follows. Firstly, the design of the TATS is introduced in Section II. The energy efficiency of the TATS is compared with the cable-suspended framework in Section III. Then in Section IV, the robustness of the TATS configuration is quantified by the capacity margin. Finally, a prototype and associated physical experimental results are given in Section IV.

II. System Description and Design

In this section, the quasi-static motion of the TATS will be analyzed to show the difference from the cable-suspended framework. Then, the principles of determining the bar-connection topology are presented for the TATS construction. Finally, a method to check the strength of bars is provided.

A. System Description

The TATS is shown in Fig. 1, where the system consists of n ($n \geq 3$) homogeneous UAVs, n cables, m bars and a mass point payload. In inertial frame, the ith UAV is located at $\boldsymbol{p}_i$ with the mass of m_U. The position of the payload is $\boldsymbol{p}_L$, whose mass is m_L. The payload connects n UAV via n cables. Bars only connect some specific pairs of UAVs' Center Of Mass (COM). The endpoints of bars link the COM of UAVs via spherical joints, whose maximum rotation is limited by $\bar{\delta}$. The attitude of each UAV can be decoupled from the truss. It is assumed that the center-axis unit vectors of spherical joints are all along the same direction of gravity, that $\boldsymbol{n}_i = \begin{bmatrix}0 & 0 & 1\end{bmatrix}^T$.

When the TATS hovers, connected bars and cables form a tensile network, which can be regarded as a truss structure. The quasi-static motion of the TATS is

$$\mathbf{W} = -\boldsymbol{G}, \tag{1}$$

where

$$\mathbf{W} = \begin{bmatrix}\mathbf{W}_1 \\ \mathbf{W}_2\end{bmatrix} = \begin{bmatrix}\boldsymbol{f}_1 & \cdots & \boldsymbol{f}_n \\ \boldsymbol{r}_1 \times \boldsymbol{f}_1 & \cdots & \boldsymbol{r}_n \times \boldsymbol{f}_n\end{bmatrix},$$
$$\boldsymbol{G} = \begin{bmatrix}m_c \boldsymbol{g} \\ 0\end{bmatrix},$$

$\boldsymbol{f}_i$ represents the thrust of ith UAV; $\boldsymbol{r}_i = \boldsymbol{p}_i - \boldsymbol{p}_c$ denote the related position from the COM of the TATS (denoted by $\boldsymbol{p}_c$) to ith UAV; m_c is the total mass of the TATS and $\boldsymbol{g}$ represents the gravity.

Due to the rotation limitation of spherical joints and the maximum thrust magnitude $f_{\max}$ of each UAV, there holds

$$\boldsymbol{f}_i^T \left[\cos^2\bar{\delta}\mathbf{I}_3 - \boldsymbol{n}_i \boldsymbol{n}_i^T\right] \boldsymbol{f}_i \leq 0, \tag{2}$$
$$\boldsymbol{f}_i^T \boldsymbol{f}_i \leq f_{\max}^2. \tag{3}$$

In view of (1), there are no horizontal force components and all of the thrusts of UAVs are used to compensate the gravity, which is benefited from the existence of inner compressive stresses such as $\boldsymbol{F}_i^{inner_1}$ and $\boldsymbol{F}_i^{inner_2}$ shown in Fig. 1. Meanwhile, as a price, some extra bars need to be added. Notice that the features of the forces on bars are all along with the axial directions of bars. Hence, those bars can be manufactured lightweight with strong resistance to axial stress, which is one of the structural superior properties of truss structures.

Remark 1: Safe flight distance is a crucial factor that must be considered in the cable-suspended framework. Especially in the environments of low-accuracy positioning. In field GPS conditions, the requirement of safe flight distance will rise further. However, the TATS is insensitive to positioning accuracy because connected bars naturally impose distance constraints on UAVs. In addition, the TATS can be designed even more compactly to meet the various task requirements.

B. TATS Construction

Assumption 2: UAVs will not collide with additional bars due to the appropriate spherical joint constraint.

The construction of a TATS can be started from a cable-suspended framework, where n cables connect n UAVs to the same payload. UAVs and the payload have been determined in the cable-suspended framework. What left for us is to

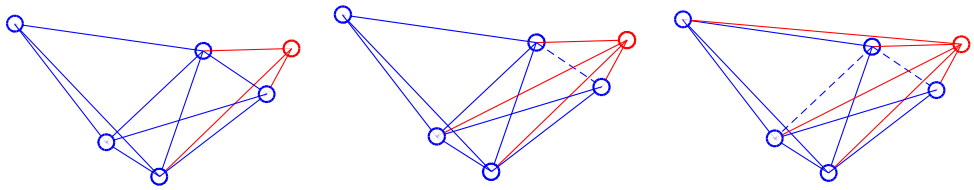

(a) (b) (c)

Fig. 2. An example of Henneberg construction. A minimally rigid graph has been constructed consisting of nodes and edges in blue. The red node is a new one to be added into the graph. (a), (b) and (c) show three feasible configurations, in which none, one, and two original edges are removed, respectively. The dashed lines in blue represent the removed original edges and the red lines are new edges.

decide which and how many pairs of UAVs require additional bar connections.

UAVs and the payload compose the node set V. Cables and additional bars form the edge set E. The topology relations among the node set V and the edge set E can be described by a graph $\mathcal{G}$. In the cable-suspended framework, it is remarked that cables are tensile under gravity so that they can be regarded as massless rigid bars. To construct a truss structure, bars, cables, and the payload need to compose a rigid body under gravity, or rather the corresponding graph $\mathcal{G}$ of the TATS must be a rigid graph.

The fewer additional bars will raise the less extra weight for the TATS, which implies a minimal rigidity [20] construction problem. A graph is minimally rigid if it is rigid and if no single interagent distance constraint can be removed without causing the formation to lose rigidity. According to Laman's theorem [21], for a rigid graph $\mathcal{G}$ in three dimensions, it is minimal rigidity if and only if $|E| = 3|V| - 6$, where $|E|$ and $|V|$ are the numbers of edges and nodes of the graph $\mathcal{G}$. For the TATS, $|V| = n + 1$, has been determined by n UAVs and the payload in the cable-suspended framework. n edges have also been determined by originally connected cables. Therefore, $m = 2n - 3$ bars are required.

Henneberg construction [20] is a technique for growing minimally rigid graphs, which starts from three noncollinear nodes and three edges joining the nodes forming a triangle. At each step, a new node and three new edges are added. Three new edges connect the new node with three noncollinear nodes in the original rigid graph. Besides, more new edges can also be added with equivalent original edges removed. For the same node addition, Fig. 2 presents one step of Henneberg construction in different feasible minimally rigid configurations. More details may refer to [14] and [20].

As for the TATS, Henneberg construction will start from two UAVs and the payload, which is connected by two cables and an additional bar. At each step, one new UAV will be selected with an original tethered cable and two additional bars, until all UAVs are included.

C. Bars Strength Check

Assumption 2: The bars are uniform, whose mass can be averagely distributed to the pair of two connected UAV nodes.

The strength of bars will be checked for a constructed TATS. There are $|V| = n + 1$ nodes and $|E| = n + m$ edges forming a minimally rigidity truss. Those all nodes and edges constitute a graph $\mathcal{G}$. The node set consists of n UAVs indexed by 1 to n and a payload indexed by $n + 1$. The edge set consists of $s = n$ cables and $m = 2n - 3$ bars. We firstly introduce two matrices for a graph.

Connectivity matrix $\mathbf{C} \in \mathbb{R}^{|E|\times|V|}$: The first s rows of $\mathbf{C}$ correspond to cable members and the rest m rows of $\mathbf{C}$ correspond to bar members. If member k connects nodes i and j $(i < j)$, the elements in k-th row of $\mathbf{C}$ are

$$\mathbf{C}(k,h) = \begin{cases} 1 & h = i \\ -1 & h = j \\ 0 & \text{else} \end{cases}.$$

Adjacency matrix $\mathbf{A} = [a_{ij}] \in \mathbb{R}^{|V|\times|V|}$: The elements of $\mathbf{A}$ are

$$a_{ij} = 1 \Leftrightarrow (\upsilon_i, \upsilon_j) \in E,$$
$$a_{ij} = 0 \Leftrightarrow (\upsilon_i, \upsilon_j) \notin E,$$

where (υ_i, υ_j) represents an edge from node j to i. For an undirected graph, $\mathbf{A}$ is symmetric.

Force Density Method (FDM) [22] can calculate equilibrium forces in a networked truss structure. Under Assumption 1, the mass of each bar can be distributed to the connected pair of UAV nodes. The mass on ith UAV node m_i can be computed as

$$m_i = m_U + \frac{1}{2}\sum_{j=1}^{n} a_{ij} m_{ij},$$

where m_{ij} is the mass of the bar connecting the node i and j.

The forces on each node include the gravity and thrust. The thrust can be computed via the equilibrium with the spherical joints limitation. The minimum power of thrusts can be given via solving the following optimization [11] :

$$\begin{aligned} \min \quad & \boldsymbol{f}^T\boldsymbol{f}, \\ \text{s.t.} \quad & (1), (2), (3), \end{aligned} \tag{4}$$

where

$$\boldsymbol{f} = \begin{bmatrix} \boldsymbol{f}_1^T & \cdots & \boldsymbol{f}_n^T \end{bmatrix}^T. \tag{5}$$

Now compute the tensile force along with edges. The kth edge is with tensile force T_k in length l_k. The force density is defined as

$$q_k = \frac{T_k}{l_k}.$$

The force equilibrium in the truss tensile network is [**?**]

$$\begin{aligned}\mathbf{C}^T diag\,(\boldsymbol{q})\,\mathbf{C}\boldsymbol{x} &= \boldsymbol{F}_x,\\ \mathbf{C}^T diag\,(\boldsymbol{q})\,\mathbf{C}\boldsymbol{y} &= \boldsymbol{F}_y,\\ \mathbf{C}^T diag\,(\boldsymbol{q})\,\mathbf{C}\boldsymbol{z} &= \boldsymbol{F}_z,\end{aligned} \tag{6}$$

where

$$\boldsymbol{q} = \begin{bmatrix} q_1 & \cdots & q_{|E|}\end{bmatrix}^T,$$

$\boldsymbol{x}$, $\boldsymbol{y}$, $\boldsymbol{z} \in \mathbb{R}^{|V|}$ represent the Cartesian coordinates for all nodes along with the respective axis; $\boldsymbol{F}_x$, $\boldsymbol{F}_y$ and $\boldsymbol{F}_z$ are the forces applied to the nodes in the x, y and z directions, respectively.

It holds that $diag\,(\boldsymbol{a})\,\boldsymbol{b} = diag\,(\boldsymbol{b})\,\boldsymbol{a}$ for two vectors $\boldsymbol{a}$ and $\boldsymbol{b}$. A compact form can be obtained from (6), yielding

$$\mathbf{H}\boldsymbol{q} = \boldsymbol{F}, \tag{7}$$

where

$$\mathbf{H} = \begin{bmatrix}\mathbf{C}^T diag(\mathbf{C}\boldsymbol{x})\\ \mathbf{C}^T diag(\mathbf{C}\boldsymbol{y})\\ \mathbf{C}^T diag(\mathbf{C}\boldsymbol{z})\end{bmatrix},$$
$$\boldsymbol{F} = \begin{bmatrix}\boldsymbol{F}_x^T & \boldsymbol{F}_y^T & \boldsymbol{F}_z^T\end{bmatrix}^T.$$

Hence, the yielding strength of bars σ should satisfy

$$\sigma > \max\left\{\chi\frac{q_k l_k}{A_k}\right\}, \tag{8}$$

where $0 < \chi < 1$ is the factor of safety for practical engineering; A_k represents the cross sectional area of kth bar.

III. ENERGY EFFICIENCY

In the construction of TATS, the gravity of the additional bars need to be compensated by extra thrusts. A comparison between the TATS and the cable-suspended framework on energy consumption will be drawn.

We consider a cable-suspended framework with a symmetric configuration. Cables are set with the same length and inclined angle ϑ. UAVs are evenly distributed on a circle. A TATS is constructed based on this symmetric cable-suspended framework.

The energy consumption during the transportation is indicated by the total magnitude of thrusts. We focus on the consumption caused by the payload and additional bars. The energy consumption of the TATS is defined as

$$\eta_1 = (m_L + m_B)\,|g|\,. \tag{9}$$

The energy consumption of the cable-suspended framework cost by the payload is defined as

$$\eta_2 = \sqrt{\left\|F^{\parallel}\right\|_2^2 + \left\|F^{\perp}\right\|_2^2} - n m_U\,|g|\,, \tag{10}$$

with

$$\begin{aligned}F^{\parallel} &= (m_L + n m_U)\,|g|\,,\\ F^{\perp} &= m_L\,|g|\tan\vartheta,\end{aligned}$$

where $F^{\parallel}$ represents the total vertical components of all thrusts; $F^{\perp}$ is the total horizontal components of all thrusts.

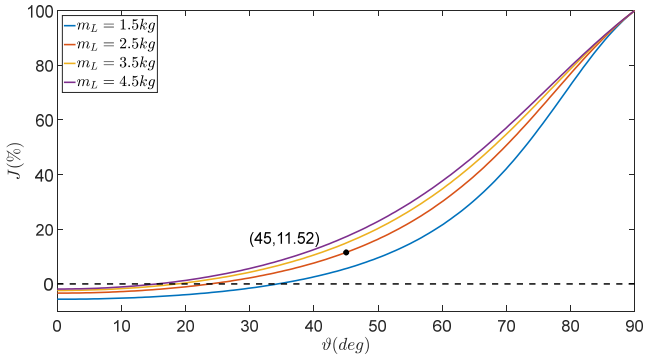

Fig. 3. The relationship among J, ϑ and m_L. Marked black point corresponds to the load test in Section V.

Compared with the cable-suspended framework, the energy consumption decrease of the TATS is defined as

$$J = 1 - \frac{\eta_1}{\eta_2}. \tag{11}$$

To ensure the decrease of energy consumption, the upper bound of bars' total mass $\overline{m}_B$ can be computed by letting $J = 0$, given by

$$\overline{m}_B = \sqrt{(m_L + n m_U)^2 + m_L^2\tan^2\vartheta} - (m_L + n m_U)\,. \tag{12}$$

It can be proved that

$$\frac{\partial J}{\partial \vartheta} > 0, \tag{13}$$

$$\frac{\partial J}{\partial m_L} > 0. \tag{14}$$

The calculation details are presented in Appendix A. It is obvious that the smaller m_B will result in less energy consumption. From (13) and (14), J is also monotonically increasing with respect to ϑ and m_L. Therefore, the larger inclined angle ϑ and the heavier payload m_L will result in more efficiency, which is also consistent with our motivation aiming for heavy payload transportation. It is shown that the TATS may not be preferable for light payloads, which has been shown in Fig 3. The curves below the dashed black line will result in inefficiency due to the gravity burden induced by the addition bars.

Remark 2: Small inclined angle ϑ is adverse to neither the TATS nor the cable-suspended framework. According to Fig. 3, Small inclined angle ϑ corresponds to little and even negative J. In the cable-suspended framework, small ϑ corresponds to configurations with low robustness [24]-[25], and in which, cables can easily become slack. If the flight distance of UAVs is fixed, the smaller inclined angle will require longer cables, yielding a large-sized transportation system.

IV. WRENCH SPACE ANALYSIS

In this section, the wrench space will be analyzed to compute the capacity margin for evaluating the robustness of the TATS configuration. We firstly introduce some necessary definitions.

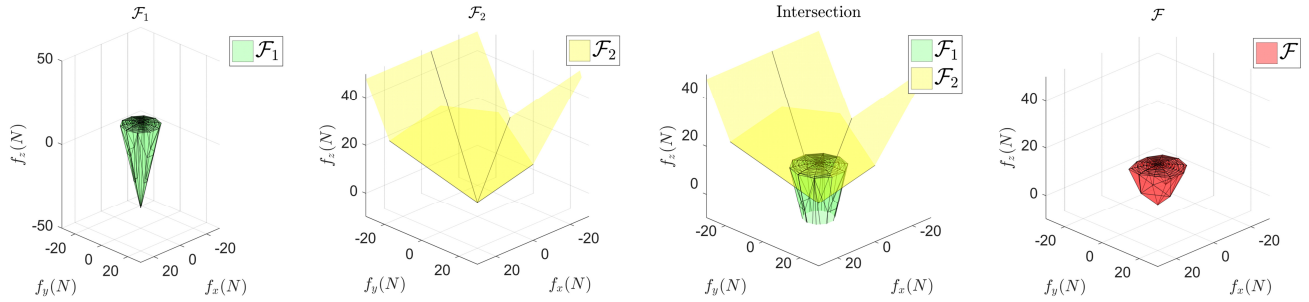

(a) $\mathcal{F}_1$ (b) $\mathcal{F}_2$ (c) $\mathcal{F}_1 \bigcap \mathcal{F}_2$ (d) $\mathcal{F}$

Fig. 4. An example of force space of the TATS. In this case, a TATS consists of three UAVs, the payload, and some proper bars.

Wrench Space [23]-[25]: The wrench space is the set of available external wrenches that the system can exert, which is determined by the system structure and actuators' capability. For 6-DOF rigid body, the wrench space consists of force space and moment space.

Capacity Margin: The capacity margin γ is an index used to evaluate the robustness of the equilibrium. It is defined as the shortest Euclidean distance from the equilibrium to the wrench space.

It is considered the external force on the payload, which also accordingly generates an external moment. How large external force on the payload can be resisted is the meaning of the TATS capacity margin.

The wrench space of the TATS is similar to the feasible control set discussed in [11]. The force space $\mathcal{F}_1$ and moment space $\mathcal{M}$ are written as

$$\mathcal{F}_1 = \mathbf{W}_1 \boldsymbol{f} + m_c \boldsymbol{g}, \tag{15}$$
$$\mathcal{M} = \mathbf{W}_2 \boldsymbol{f}, \tag{16}$$

with constraint (2) and (3).

As shown in Fig. 4(a), $\mathcal{F}_1$ is a cone, whose cone angle is related to the maximum rotation angle $\overline{\delta}$ of spherical joints and its height relates to the maximum thrust magnitude $f_{\max}$ of UAVs.

Note that the external force can never destroy the rigid structure of trusses. To be specific, all cables should be in tension, which introduces an additional constraint to the force space $\mathcal{F}_1$. For the payload node, all admissible external force will be compensated by the tension on those connected cables. Under this constraint, the available external force set is

$$\mathcal{F}_2 = \mathbf{W}_3 \boldsymbol{t} + m_L \boldsymbol{g}, \tag{17}$$

subject to $t_i > 0$, where

$$\mathbf{W}_3 = \begin{bmatrix} \boldsymbol{v}_1 & \cdots & \boldsymbol{v}_n \end{bmatrix},$$
$$\boldsymbol{t} = \begin{bmatrix} t_1 & \cdots & t_n \end{bmatrix}^T,$$

$\boldsymbol{v}_i = (\boldsymbol{p}_i - \boldsymbol{p}_L)/\|\boldsymbol{p}_i - \boldsymbol{p}_L\|_2$ represents the direction of ith cable. t_i is the tension magnitude of ith cable. $\mathcal{F}_2$ is presented in Fig. 4(b).

Hence, the force space associated with the external force on the payload is an intersection $\mathcal{F} = \mathcal{F}_1 \bigcap \mathcal{F}_2$, which can be found in Fig. 4(c). The resulting force space $\mathcal{F}$ is presented in Fig. 4(d).

Notice that the units of force space $\mathcal{F}$ and moment space $\mathcal{M}$ are different. The moment is generated by the external force on the payload. Therefore, the moment space can be homogenized by dividing the characteristic distance $r = \|\boldsymbol{p}_L - \boldsymbol{p}_c\|_2$ [25]. The homogenized moment space $\bar{\mathcal{M}}$ is derived as

$$\bar{\mathcal{M}} = \mathbf{W}_2 \boldsymbol{f}/r. \tag{18}$$

Finally, the capacity margin can be obtained by

$$\gamma = \min\left\{\gamma_{\mathcal{F}}, \gamma_{\bar{\mathcal{M}}}\right\}, \tag{19}$$

where $\gamma_{\mathcal{F}}$ and $\gamma_{\bar{\mathcal{M}}}$ are the capacity margin computed by force space $\mathcal{F}$ and homogenized moment space $\bar{\mathcal{M}}$, respectively.

V. PROTOTYPE AND EXPERIMENT

In this section, a TATS prototype and its load test will be presented.

A. Mechanics

Assembling more than one articulated connection into a single component requires complex mechanical design, and leads to heavy weights. According to the analysis in Section III, the truss should be as light as possible. Hence, in our prototype, multiple spherical joint buckles are connected to a single component, which is shown in Fig. 5. The maximum rotation angle of bar-connected spherical joint buckles can be designed small, because bars and cables keep a rigid truss structure during transportation. With the help of resin material, the weight of one articulated node is only 3g.

B. Prototype

A TATS prototype, shown in Fig. 6, consists of four quadrotor UAVs, four cables, five carbon fiber bars, and four articulated components.

The weight of a quadrotor UAV is 1.18kg with a wheelbase 250mm. Each UAV is equipped with a PX4[1] flight control system and an NVIDIA Jetson Xavier NX[2] onboard processor. Each of the four T-motor F40 Pro motors can provide a maximum thrust of 56N in total.

[1]https://px4.io/

[2]https://developer.nvidia.com/embedded/jetson-xavier-nx

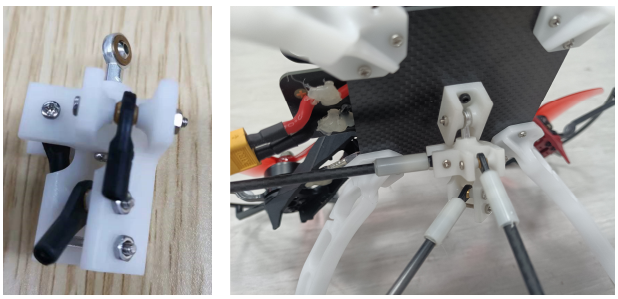

(a) Articulated component. (b) Assembled articulated component.

Fig. 5. Articulated component.

Fig. 6. Prototype of the TATS.

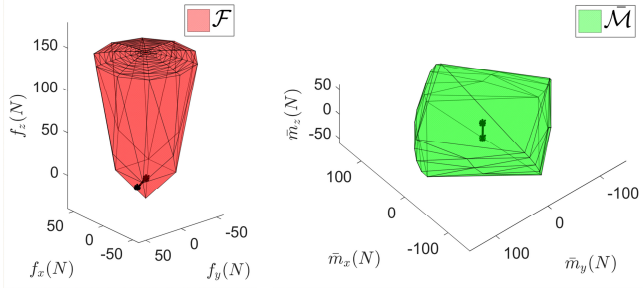

(a) Force space. (b) Homogenized moment space.

Fig. 7. Wrench space of prototype, where the black solid lines are the shortest distance form the equilibrium to the force space and homogenized moment space.

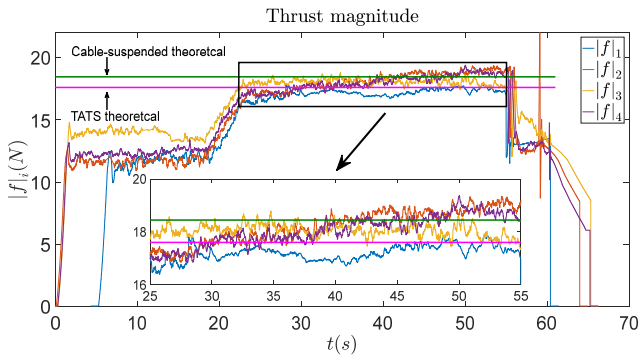

Fig. 8. Thrust magnitude of UAVs in load experiment.

The diameter of five hollow carbon fiber bars is 4mm. Four of them are 0.6m in length and the rest is 0.8485m. The payload is tethered by four cables of length 0.6m. It can be found in Fig. 6 that those elements constitute a symmetric square pyramid truss structure, whose connection topology is minimally rigid. The total mass of these elements for constructing the truss structure is only 80.4g.

According to the above mentioned geometric parameters of the prototype, the inclined angle is computed $\vartheta = \frac{pi}{4}$ rad. The payload with a mass of 2.5kg is employed in the load test. Following the FDM in Section III.C, it is computed that the maximum stress on a bar in our prototype is 1.66N. According to our material test, the bar with the maximum length of 0.8485m can resist stress more than 10N. The safety factor is selected $\chi = 0.7$. It has 10N$*$0.7 = 7N$>$ 1.66N. Therefore, the structural strength of the truss fully meets the requirement.

C. Wrench Space and Capacity Margin

Following the method in Section IV, the homogenized moment space is presented in Fig. 7(a), and the force space in Fig. 7(b). The black lines represent the shortest Euclidean distance from the equilibrium to the homogenized moment and force space, where $\gamma_{\bar{\mathcal{M}}} = 30.3142$N and $\gamma_{\mathcal{F}} = 14.1451$N, respectively. Hence, the capacity margin of our prototype TATS is $\gamma = \min\{\gamma_{\mathcal{F}}, \gamma_{\bar{\mathcal{M}}}\} = 14.1451$N.

D. Load Test

The load test of our TATS prototype is conducted with the help of OptiTrack[3] positioning system. The thrust magnitude curve of UAVs during the experiment is presented in Fig. 8. The pink line represents the theoretical thrust magnitude to lift the payload, which is computed by evenly distributing the total mass of the TATS to each UAV. The result is calculated as $f_{TATS} = 17.59$N.

As observed from the experimental result, all UAVs have taken off before 6s. After a short period of hovering, UAVs begin to rise. When the payload leaves the ground, tethered cables become tensile, meanwhile, the truss structure is formed. During the 23s-55s, UAVs are hoisting and transporting the payload. The average thrust during this period is calculated and compared with the theoretical value in Table I. With the high-precision positioning system OptiTrack, deviations between the experimental result and the theoretical value are slight, which are all less than 4%. It supports the correctness of the theoretical model analysis.

TABLE I

THRUSTS MAGNITUDE IN EXPERIMENT.

	UAV1	UAV2	UAV3	UAV4
Average thrust magnitude (N)	17.15	18.15	17.60	17.54
Deviation from theoretical (%)	2.50	-3.16	-0.05	0.28

In Fig. 8, the green line is the computed thrust magnitude of the original cable-suspended framework, $f_{cable} = 18.44$N. Following the energy efficiency computing method

[3]https://www.optitrack.com/

in Section III, it is obtained that $J = 11.52\%$, which implies the prototype TATS saves 11.52% energy in this transportation task. It also corresponds to the marked black point in Fig. 3.

VI. CONCLUSION

In this work, a new aerial cooperative transportation system TATS has been proposed, which integrates the structural advantage of truss and rigid framework. The TATS has high efficiency and compact volume, which is especially suitable for small but heavy payloads. We have also made a prototype following the proposed design steps and construction method. Then the theoretical analysis is carried out in terms of the wrench space to calculate the corresponding. It follows from the experiment on our prototype that 11.52% energy can be saved compared with the same configurated cable-suspended framework, which shows the high energy efficiency of the proposed TATS structure.

APPENDIX

A. Computation of Partial Derivative

It is complex to directly compute the partial derivative $\partial J/\partial \vartheta$ and $\partial J/\partial m_L$. We consider

$$\frac{\partial \eta_1}{\partial \vartheta} = 0,$$
$$\frac{\partial \eta_2}{\partial \vartheta} = \frac{m_L^2 \tan\vartheta \left(\tan^2\vartheta + 1\right)}{\sqrt{m_L^2 \tan^2\vartheta + (m_L + n m_U)^2}} |g| > 0.$$

Thus, $\partial J/\partial \vartheta > 0$.

Similarly,

$$\frac{\partial \eta_1}{\partial m_L} = |g|,$$
$$\frac{\partial \eta_2}{\partial m_L} = \sqrt{2}\frac{m_L + n m_U + m_L \tan^2\vartheta}{\sqrt{m_L^2 \tan^2\vartheta + (m_L + n m_U)^2}} |g| > |g|.$$

We have $\partial J/\partial m_L > 0$.

ACKNOWLEDGMENT

This work was supported in part by the Natural Science Foundation of China (NSFC) under Grants 61903035, 62133002, U1913602, 62073035, 61873033, 62088101, in part by the Shanghai Municipal Science and Technology Major Project (2021SHZDZX0100), and in part by the Beijing Advanced Innovation Center for Intelligent Robots and Systems, Beijing Institute of Technology, China.

REFERENCES

[1] G. Skorobogatov, C. Barrado, and E. Salam, "Multiple UAV Systems: A Survey," *Unmanned Syst.*, vol. 8, no. 2, pp. 149-169, 2020.

[2] Q. Song, Y. Zeng, J. Xu, and S. Jin, "A survey of prototype and experiment for UAV communications," *Sci. China Inf. Sci.*, vol. 64, no. 4, 2021.

[3] N. Michael, J. Fink, and V. Kumar, "Cooperative manipulation and transportation with aerial robots," *Auton. Robot.*, vol. 30, no.1, pp. 7386, Jan. 2011.

[4] J. Geng and J. W. Langelaan, "Cooperative transport of a slung load using load-leading control," *J. Guid. Control. Dyn.*, vol. 43, no. 7, pp. 1313-1331, Jul. 2020.

[5] B. E. Jackson, T. A. Howell, K. Shah, M. Schwager and Z. Manchester, "Scalable Cooperative Transport of Cable-Suspended Loads With UAVs Using Distributed Trajectory Optimization," *IEEE Robot. Autom. Lett.*, vol. 5, no. 2, pp. 3368-3374, Apr. 2020.

[6] G. Tartaglione, E. DAmato, M. Ariola, P. S. Rossi and T. A. Johansen, "Model predictive control for a multi-body slung-load system," *Robot. Auton. Syst.*, vol. 92, pp. 1-11, Jun. 2017.

[7] H. G. d. Marina and E. Smeur, "Flexible collaborative transportation by a team of rotorcraft," in *Proc. Int. Conf. Robot. Autom.*, May 2019, pp. 1074-1080.

[8] X. Zhang, F. Zhang, P. Huang and et al., "Self-Triggered Based Coordinate Control With Low Communication for Tethered Multi-UAV Collaborative Transportation," *IEEE Robot. Autom. Lett.*, vol. 6, no. 2, pp. 1559-1566, Apr. 2021.

[9] J. Wehbeh, S. Rahman, and I. Sharf, "Distributed Model Predictive Control for UAVs Collaborative Payload Transport," in *Proc. IEEE/RSJ Int. Conf. Intell. Robots Syst.*, Oct. 2020, pp. 11666-11672.

[10] Y. H. Tan, S. Lai, K. Wang, and B. M. Chen, "Cooperative control of multiple unmanned aerial systems for heavy duty carrying," *Annu. Rev. Control*, vol. 46, pp. 44-57, Apr. 2018.

[11] H. N. Nguyen, S. Park, J. Park, and D. Lee, "A Novel Robotic Platform for Aerial Manipulation Using Quadrotors as Rotating Thrust Generators," *IEEE Trans. Robot.*, vol. 34, no. 2, pp. 353-369, Apr. 2018.

[12] I. Iriarte, E. Otaola, D. Culla, I. Iglesias, J. Lasa, and B. Sierra, "Modeling and control of an overactuated aerial vehicle with four tiltable quadrotors attached by means of passive universal joints," in *Proc. Int. Conf. Unmanned Aircr. Syst.*, Sep. 2020, pp. 1748-1756.

[13] I. Hrazmi, J. Averseng, J. Quirant, and F. Jamin, "Deployable double layer tensegrity grid platforms for sea accessibility," *Eng. Struct.*, vol. 231, no. 15, Mar. 2021.

[14] B. D. O. Anderson, B. F. C. Yu, and J. M. Hendrickx, "Rigid graph control architectures for autonomous formations," *IEEE Control Syst. Mag.*, vol. 28, no. 6, pp. 48-63, Dec. 2008.

[15] C. Paul, F. J. Valero-Cuevas, and H. Lipson, "Design and control of tensegrity robots for locomotion," *IEEE Trans. Robot.*, vol. 22, no. 5, pp. 944-957, 2006.

[16] J. Friesen, A. Pogue, T. Bewley, M. De Oliveira, R. Skelton, and V. Sunspiral, "DuCTT: A tensegrity robot for exploring duct systems," in *Proc. Int. Conf. Robot. Autom.*, May 2014, pp. 4222-4228.

[17] M. Vespignani, J. M. Friesen, V. Sunspiral, and J. Bruce, "Design of SUPERball v2, a Compliant Tensegrity Robot for Absorbing Large Impacts," in *Proc. IEEE/RSJ Int. Conf. Intell. Robots Syst.*, Oct. 2018, pp. 2865-2871.

[18] J. M. Friesen, J. L. Dean, T. Bewley, and V. Sunspiral, "A Tensegrity-Inspired Compliant 3-DOF Compliant Joint," in *Proc. Int. Conf. Robot. Autom.*, May 2018, pp. 3301-3306.

[19] J. Zha, X. Wu, J. Kroeger, N. Perez, and M. W. Mueller, "A collision-resilient aerial vehicle with icosahedron tensegrity structure," in *Proc. IEEE/RSJ Int. Conf. Intell. Robots Syst.*, Oct. 2020, pp. 1407-1412.

[20] T.-S. Tay and W. Whiteley, "Generating Isostatic Frameworks," *Structural Topology*, vol. 11. pp. 21-69, 1985.

[21] G. Laman, "On graphs and rigidity of plane skeletal structures," *J. Eng. Math.*, vol. 4, no. 4, pp. 331-340, Oct. 1970.

[22] A. P. Sabelhaus et al., "Inverse Statics Optimization for Compound Tensegrity Robots," *IEEE Robot. Autom. Lett.*, vol. 5, no. 3, pp. 3982-3989, 2020.

[23] S. Bouchard, C. Gosselin, and B. Moore, "On the ability of a cable-driven robot to generate a prescribed set of wrenches," *J. Mech. Robot.*, vol. 2, no. 1, pp. 1-10, 2010.

[24] Y. Liu, F. Zhang, P. Huang, and X. Zhang, "Analysis, planning and control for cooperative transportation of tethered multi-rotor UAVs," *Aerosp. Sci. Technol.*, vol. 113, pp. 106673, Jun. 2021.

[25] J. Erskine, A. Chriette, and S. Caro, "Wrench Analysis of Cable-Suspended Parallel Robots Actuated by Quadrotor Unmanned Aerial Vehicles," *J. Mech. Robot.*, vol. 11, no. 2, Apr. 2019.